

See discussions, stats, and author profiles for this publication at: <https://www.researchgate.net/publication/321058719>

Influence of Types of Discrete Modelling of Fasteners in FEM Models

Conference Paper · June 2017

CITATIONS

7

READS

2,654

3 authors, including:



Rodrigo De Sá Martins

Federal University of Technology - Paraná/Brazil (UTFPR)

13 PUBLICATIONS 8 CITATIONS

SEE PROFILE

Some of the authors of this publication are also working on these related projects:



Fastener stiffness evaluation [View project](#)



Topology optimization of conveyor belt rollers [View project](#)

Influence of Types of Discrete Modelling of Fasteners in FEM Models

Eng. R. Martins, Prof. Dr. -Ing. Ernani Sales Palma, Mr. A. Lorentz
(*Universidade Federal de Minas Gerais, Brazil*)

Abstract

During the last few decades, many studies have been made to better describe the behavior of the load distribution in a joint. This is especially important when dealing with fatigue and a joint between composite materials, in which there is no load redistribution after yield (in contrast to metals). The first studies consider the fastener as a single spring and therefore, all models use the axial stiffness of an axial rod (EA/L), since in the case of pure tension, a fastener behaves as an axial rod. The bending stiffness is usually neglected and the transversal stiffness varies significantly from one method to another, as it is affected by installation, *i.e.*, if the joint is bolted or riveted, the level of interference, *etc.*

In 1971, Swift wrote a generic expression for the stiffness of single shear joints. This formula was widely used in the aerospace industry even for other configurations than single shear joints. In 1986, Huth performed a series of experiments and developed a more complex method that could consider the nature of the joint (riveted or bolted), a correction for double shear and other factors. The most detailed study available was performed by Morris in 2004. It incorporated important aspects of the method used by Huth and obtained a formula that considered the number of rows, width, hole expansion, pitch and Young's modulus in the thickness direction. This work is also important since it preserved all raw data, facilitating future work. The application of all those equations in a finite element model is made through a single spring between two plates of solid elements. When three or more sheets are joined, the representation is no longer equal to the one that was tested and in the case of composite materials, when using those models that were developed for metals, adaptations must be made, such as calculating the stiffness with equivalent elasticity moduli.

In contrast to the empirical methods, Rutman presented a series of papers, replacing the single spring models by a fastener composed by a series of elements that are present in NASTRAN. The combination of their properties can prevent some non-physical phenomena that occur in the single spring model.

The main objective of this paper is to briefly show the assumptions inherent to most of the models used in the aerospace industry and show which one of those is more suitable for each structural joint and load distribution.

1. Fastener modelling in finite elements

When dealing with large structures, such as an aircraft wing, it is common to model the structure with finite elements in a very crude and global way, as shown in Figure 1.

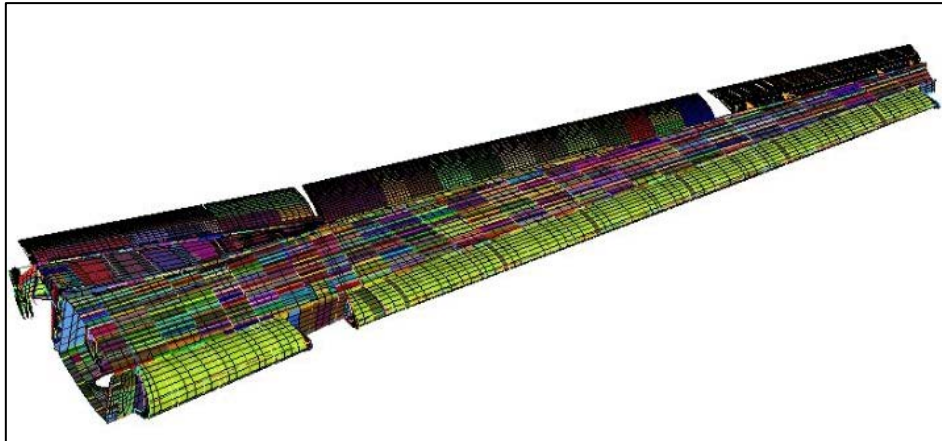


Figure 1: Global model of an airplane wing

The load in the fastening is computed either by the shear flow between elements or by free-body diagrams. This method allows you only to obtain an average value load and it is not acceptable when dealing with fatigue or composite materials.

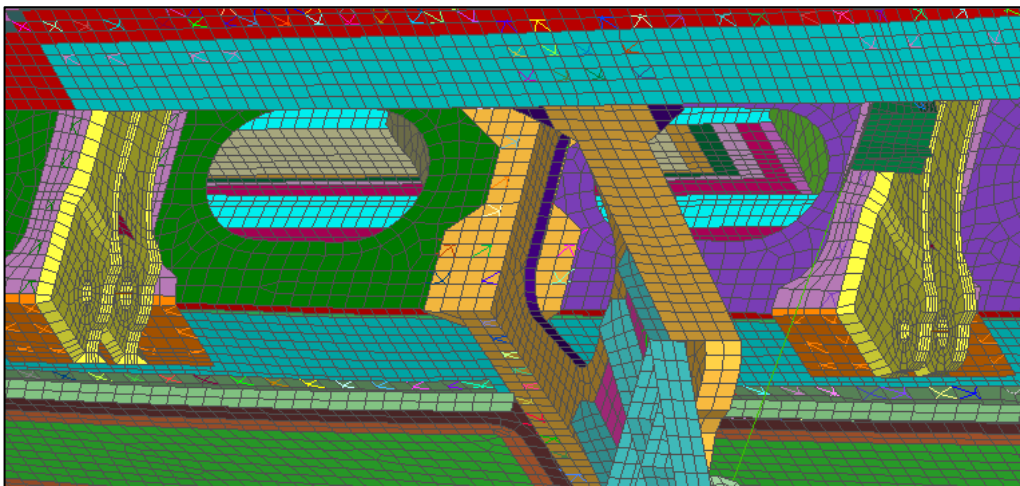


Figure 2: Detailed model of an elevator attachment

In the second case, the load in the fastener can be directly read from the fastener element. Each plate element is modelled in the midsurface of the thickness, so the fastener has a length of the sum of the thicknesses divided by

two. Sometimes this approach can lead to unrealistic results as shown in Figure 3.

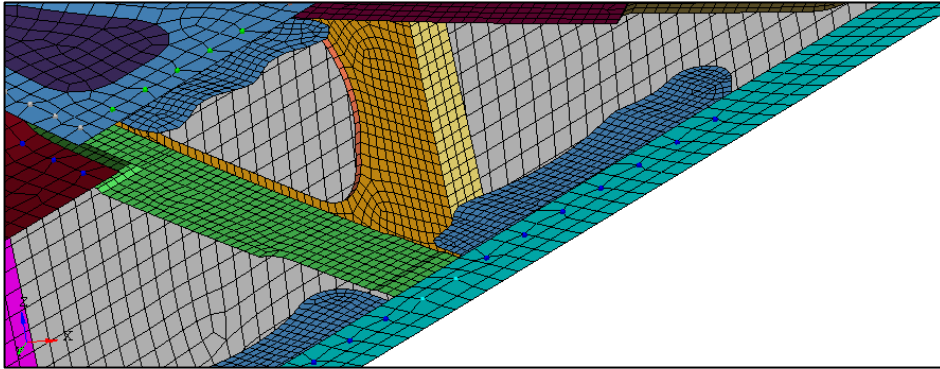


Figure 3: Detailed model of an elevator attachment

The fastening modelling of the Rib in the lower Spar Cap can lead to excessive bending moment. To prevent this effect, the nodes of the Ribs can be placed in the same plane of the fastening, or by using a modelling technique described below:

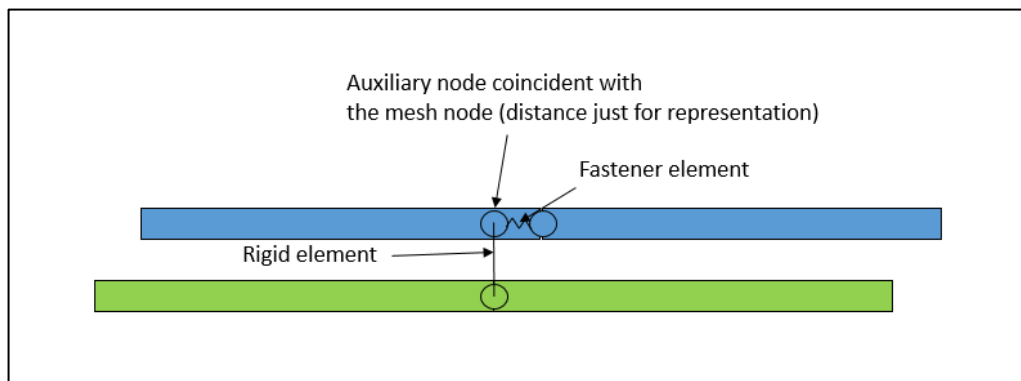


Figure 4: Rigid element fastening model technique

There is a fourth technique to model fasteners using springs when the nodes are in the same plane. This technique is useful when it is needed to prevent the unrealistic secondary moment but also it is necessary to maintain the structure flexural stiffness. It is shown in Figure 5.

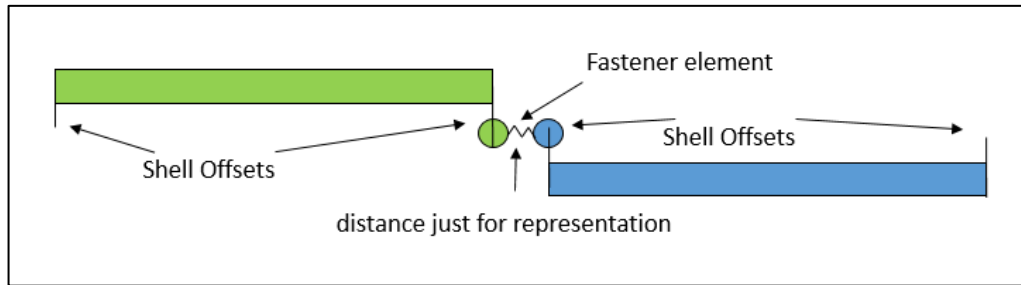


Figure 5: Shell offset technique

By placing an offset in both shell elements, it is possible to maintain the flexural stiffness of the structure, while keeping the nodes coincident.

2. Definition of flexibility

Huth defines flexibility as:

$$f = \frac{\delta}{F} \quad (1)$$

Where:

δ is the total joint displacement.

F is the applied force.

Researchers have traditionally determined expressions for flexibility rather than stiffness for the joints. This can be explained by the fact that a joint is basically one structural element connected to another, so the inverse rule of equivalent stiffness is applicable.

$$\frac{1}{k_{eq}} = \frac{1}{k_1} + \frac{1}{k_2} \quad (2)$$

In finite elements, the models use the stiffness of the element as input, therefore, it is necessary to invert the results of the formulas before using them.

Morris developed analytically an expression to find the flexibility in a lap joint with n rows of rivets. The assumption is basically that, the sheets displacement can be found by using simple elasticity. The rest of the displacement must be of the joint itself.

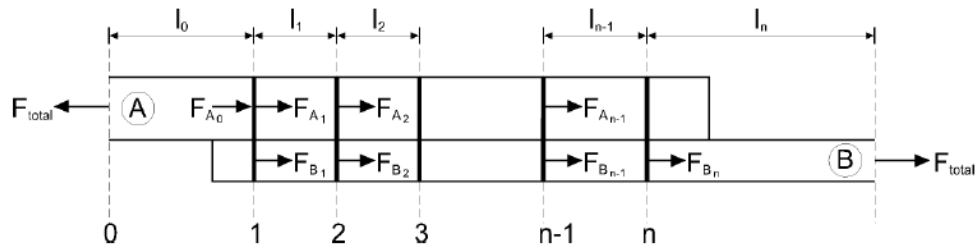


Figure 6: Model of joint for determining flexibility.

For two identical sheets with two rows of rivets as show in Figure 7 the expression is:

$$f = 2 \left(\frac{\delta_{total}}{F_{total}} - \frac{l_0 + \frac{1}{2} l_1 + l_2}{EA} \right) \quad (3)$$

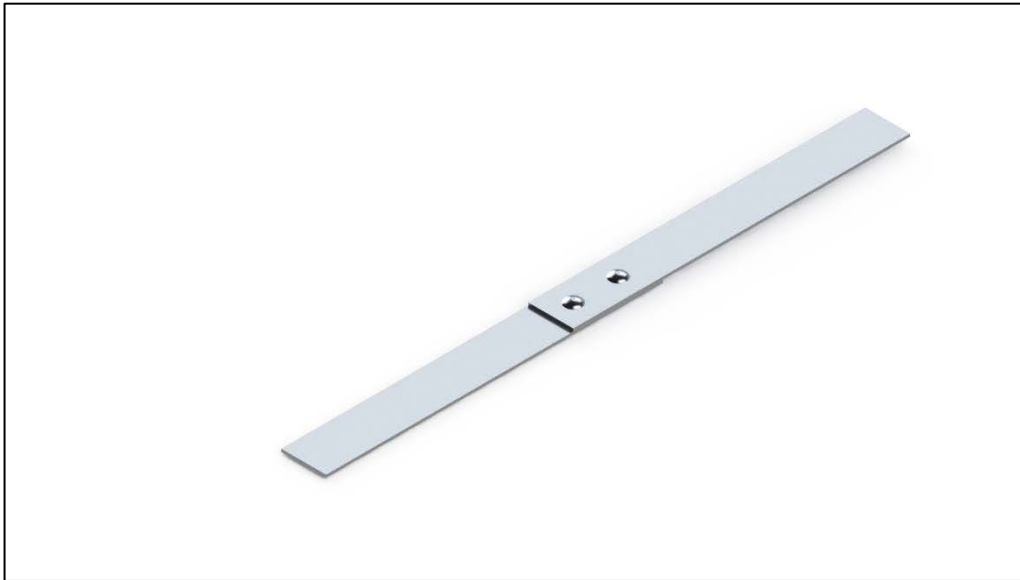


Figure 7: Model of a lap joint with two rows of rivets (one rivet in each row).

E is the Young's modulus of the sheets.

A is the cross section area.

This configuration will be widely used along the paper to compare the differences between equations and modelling.

3. Empirical Equations

Along the years, many expressions were developed to predict the flexibility of a joint. The ones that will be analyzed are:

- Swift:

$$f = \frac{5}{dE_f} + 0.8 \left(\frac{1}{t_1 E_1} + \frac{1}{t_2 E_2} \right) \quad (4)$$

As the equation (4) shows, the fastener diameter, thickness of each sheet and Young's modulus of the members are considered.

- Grumman

Both Grumman and Swift considered the same set of parameters to determine the fastening flexibility, but ended up with different expression.- In the Swift equation, the flexibility tends to be lower.

$$f = \frac{(t_1 + t_2)^2}{E_f d^3} + 3.7 \left(\frac{1}{t_1 E_1} + \frac{1}{t_2 E_2} \right) \quad (5)$$

- Huth

$$f = \left(\frac{t_1 + t_2}{2d} \right)^a \frac{b}{n} \left(\frac{1}{t_1 E_1} + \frac{1}{nt_2 E_2} + \frac{1}{nt_1 E_f} + \frac{1}{2nt_2 E_f} \right) \quad (6)$$

Huth tested several configurations of joints, such as single shear and double shear, as well as different types of fasteners.

The n is the number of planes of shear and the a and b refers to the type of fastening.

Group I – Bolted Metallic Joints	$a=2/3$	$b=3.0$
Group II – Riveted Metallic Joints	$a=2/5$	$b=2.2$
Group III – Bolted graphite/epoxy joints	$a=2/5$	$b=2.2$

- Tate and Rosenfelt

$$f = \frac{1}{E_f t_1} + \frac{1}{E_f t_2} + \frac{1}{E_1 t_1} + \frac{1}{E_2 t_2} + \frac{32}{9E_f \pi d^2} (1 + \nu_f)(t_1 + t_2) + \frac{8}{5E_f \pi d^4} (t_1^3 + 5t_1^2 t_2 + 5t_1 t_2^2 + t_2^3) \quad (7)$$

Tate and Rosenfelt could put the influence of the Poisson's ratio in the expression for the flexibility.

- Morris

Morris completed a very rigorous theoretical and experimental study on lap joints and could incorporate in his study various parameters such as rows of rivets, size of the head, Young's modulus in the thickness direction, etc.

$$f = \left(\left(\frac{2845}{E_{L1} t_1} + \frac{2845}{E_{L2} t_2} \right) + c_f \left(\left(\frac{500}{E_f t_1} + \frac{1000}{E_{ST1} t_1} \right) \left(\frac{t_1}{d} \right)^2 + \left(\frac{500}{E_f t_2} + \frac{1000}{E_{ST2} t_2} \right) \left(\frac{t_2}{d} \right)^2 \right) \right) \left(\frac{d_{head}}{d} \right)^{-0.34} \left(\frac{s}{d} \right)^{-0.5} \left(\frac{p}{d} \right)^{0.34} e^{0.3r} \quad (8)$$

Varying the parameters of each equation and inverting the result in order to obtain the stiffness of the joint, a more comprehensive understanding of each equation can be achieved.

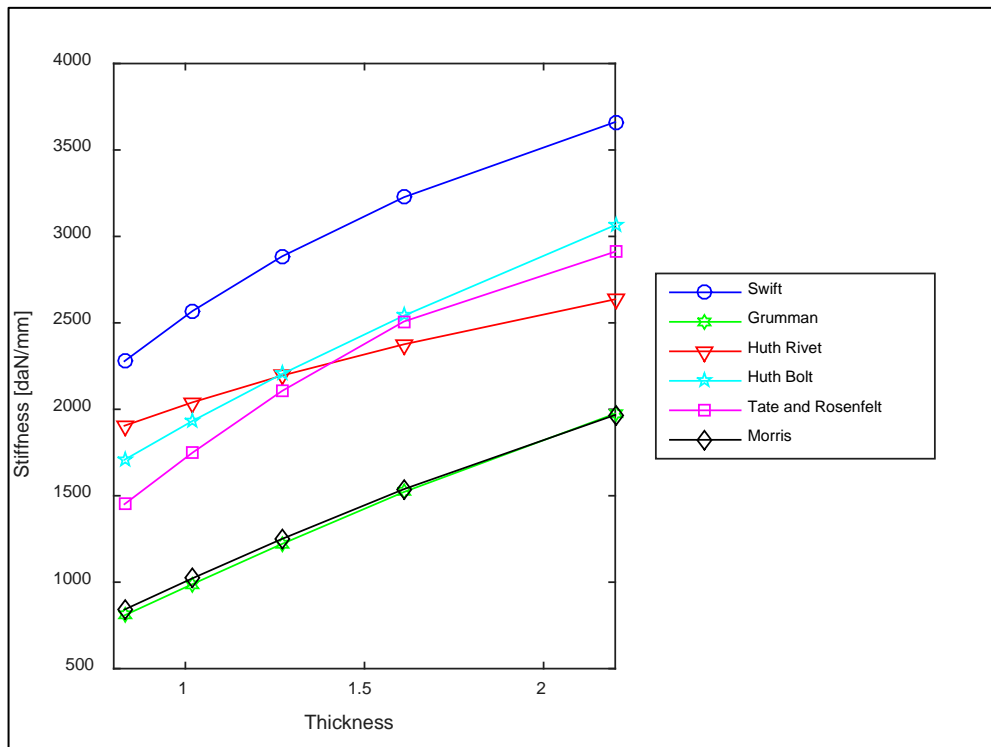


Figure 8: Variation of the fastening stiffness with the sheet thickness

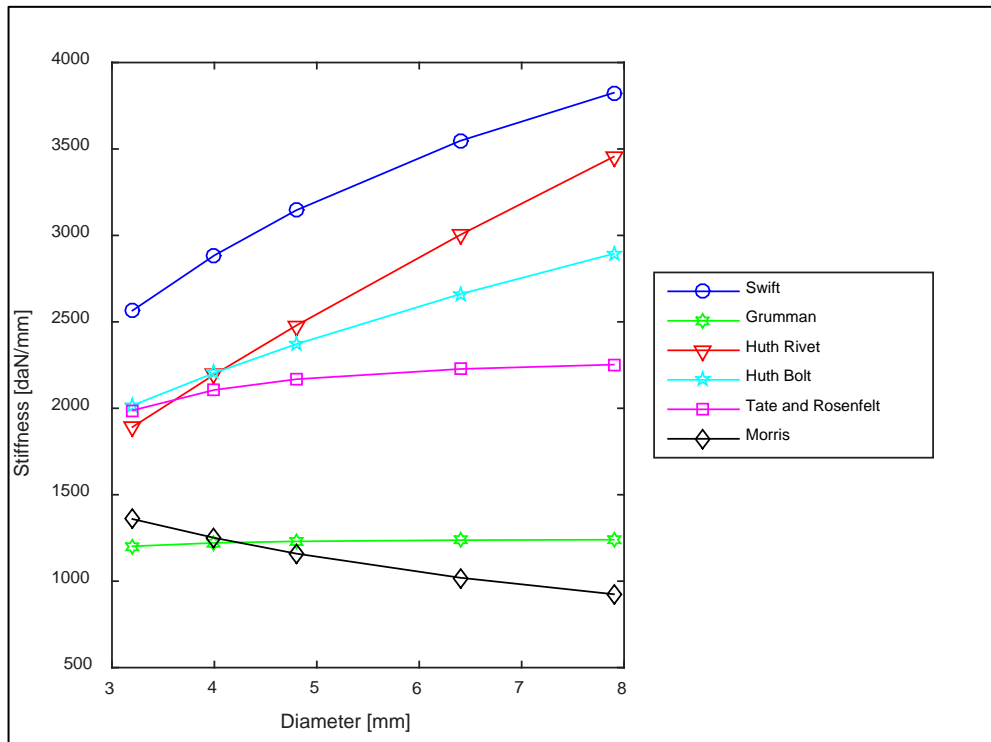


Figure 9: Variation of the fastening stiffness with the fastener diameter.

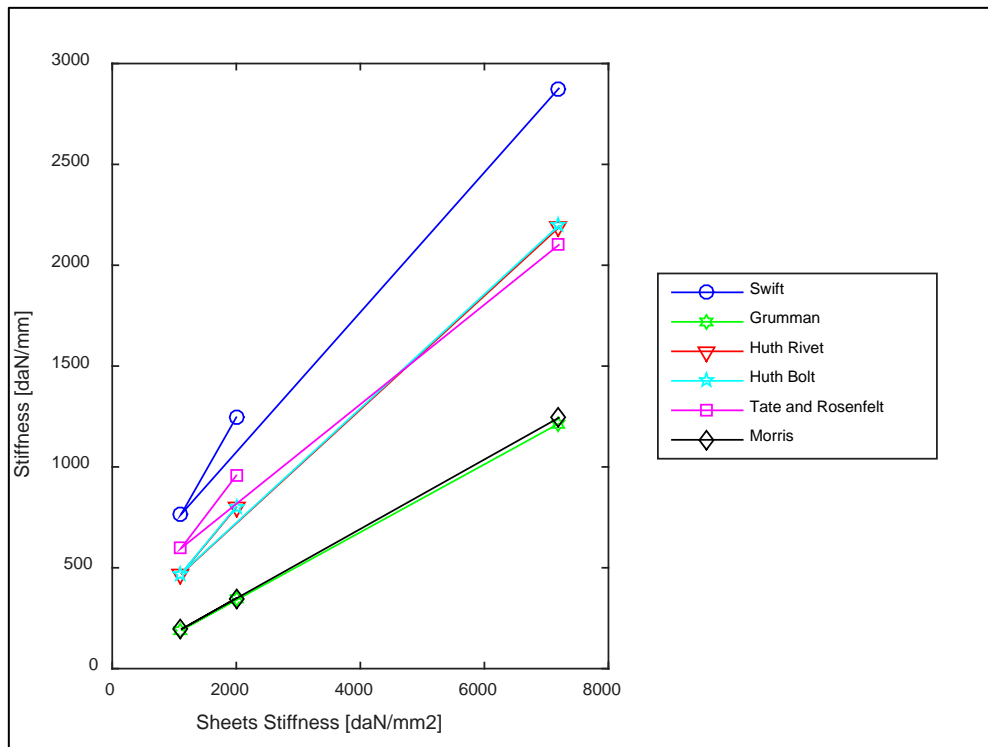


Figure 10: Variation of the fastening stiffness with the sheet Young's Modulus.

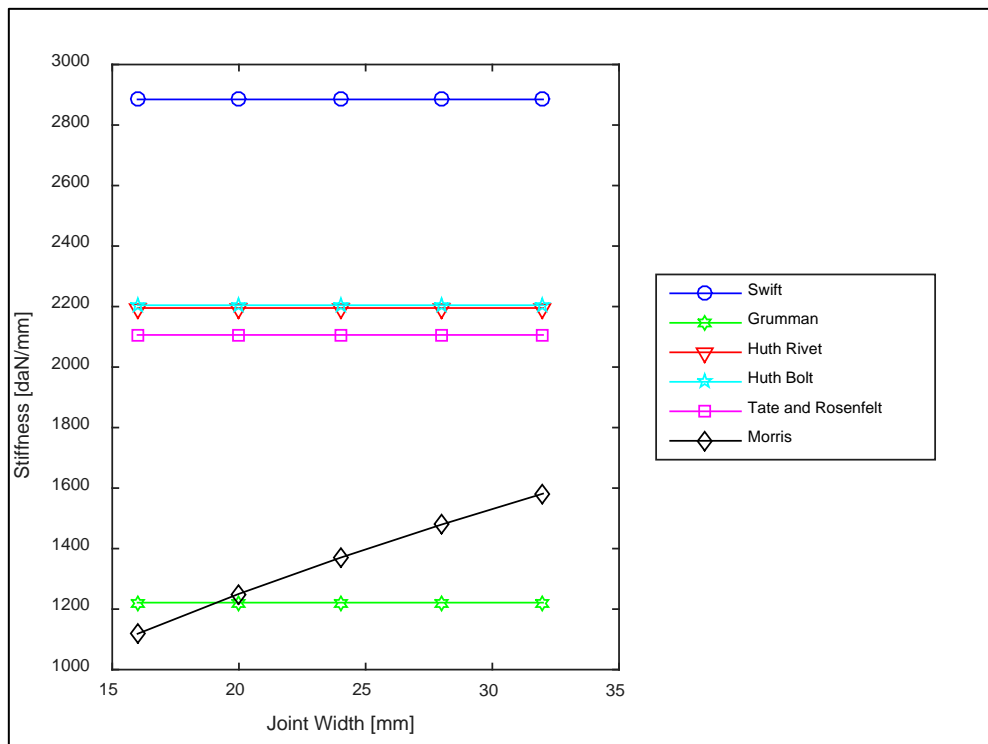


Figure 11: Variation of the fastening stiffness with the joint width.

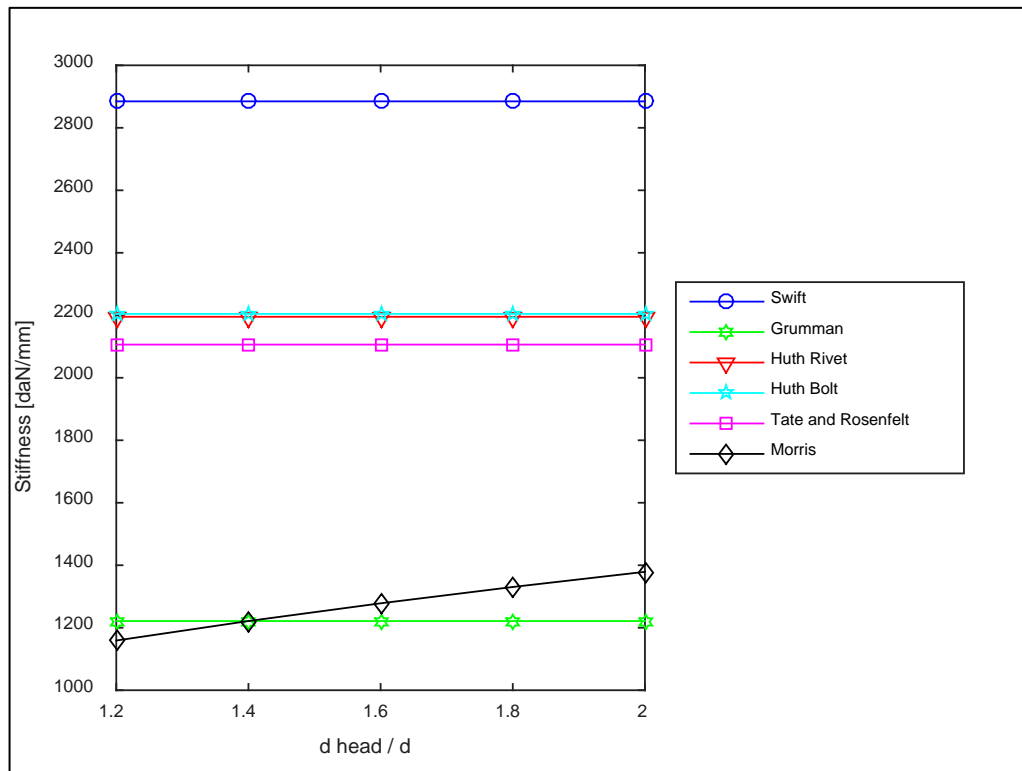


Figure 12: Variation of the fastening stiffness with the ratio between head and shank diameter.

As shown from Figure 8 to Figure 11 and also equations (4) to (8), Morris equation takes into account much more parameters. By analyzing the figures, even though Grumman has a simpler equation, the results are closer to Morris which is a much more robust equation.

4. Multi-Spring Methods

The multi-spring modelling method, created by Alexander Rutman, is one of the most used ones in the aerospace industry and presents several advantages when compared to others.

The most significant advantage comes from the fact that it can be used for any joint, with any number of joined elements.

The proposed modelling technique differs from the traditional approach, in which all the connected plates are modelled coplanar, consisting in calculating a single spring rate for a combination of fastener and plate properties. The application of the empirical approach is limited to single shear joints of two plates or symmetric double shear joints of three plates. It cannot be used for other joint configurations or joints with a larger number of connected plates. The Rutman procedure is free of those limitations.

However, Rutman did not validate his findings through experiments. In the section 6, a tentative validation is made through the tests performed by Morris.

In the Rutman modelling technique, described using the NASTRAN software, the fastener is represented by a CBAR element and the bearing contact with the sheets is represented by a BUSH element.

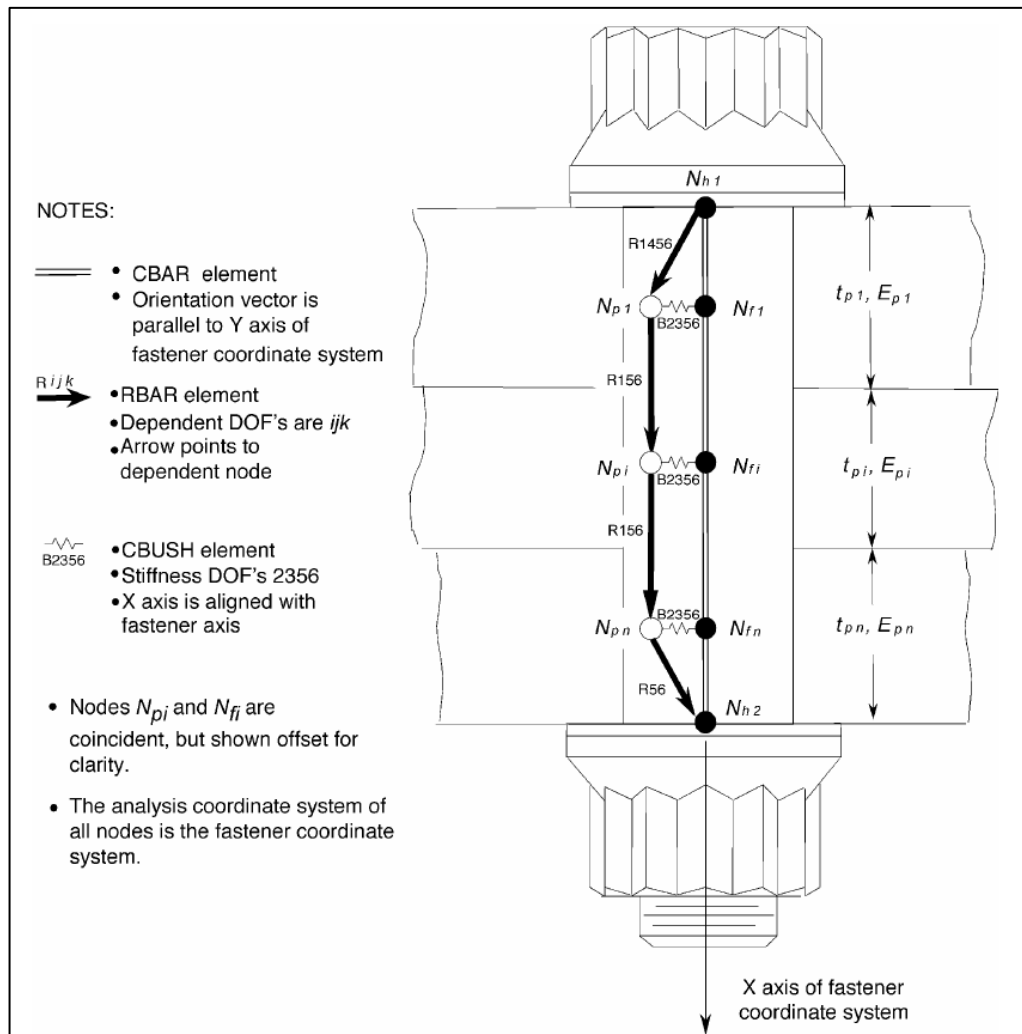


Figure 13: Rutman Fastener

All elements must be referred to the fastener coordinate system. The CBAR element represents the fastener. It has nodes for itself, separated from the shell nodes but at the same location. After the first and the last plate, there is an auxiliary element that represents the head or the nut of the fastener. The CBUSH transfers the load from the sheet to the fastener and has both shear and flexural stiffness. The black arrows are rigid elements. The arrows prevent one sheet to have rotational compatibility in the fastening point. The degree of freedom 1 between the sheets must be changed by a CGAP element (a linear contact element), so that the modelling can represent the contact between one plate and the other.

If the model is made exactly like Figure 13, the BAR does not withstand axial loads, because of the rigid element.

The stiffness of the CBUSH in directions 2 and 3 (bearing), is:

$$k_{bearing} = k_2 = k_3 = \frac{t_p}{\frac{1}{E_{cp}} + \frac{1}{E_{cf}}} \quad (9)$$

The stiffness of the CBUSH in directions 5 and 6 (bending), is:

$$k_{bending} = k_5 = k_6 = \frac{t_p^3}{12 \left(\frac{1}{E_{cp}} + \frac{1}{E_{cf}} \right)} \quad (10)$$

Where:

t_p is the plate thickness.

E_{cp} is the plate Young's modulus in compression.

E_{cf} is the fastener Young's modulus in compression.

There is no actual flexibility for the whole fastener as defined by Huth. An equivalence with the provisions section can only be made with a finite element model test. This task will be performed in the next section.

5. Numerical Experiments

In this section a numerical experiment was performed using NASTRAN. It is a lap joint test, as performed by Morris. The test parameters are shown in Table 1.

Table 1: Parameters of the test

<i>Parameter</i>	<i>Value</i>
<i>Sheet 1 material</i>	2024-T3 ($E_{L_1} = 7240 \text{ daN/mm}^2$)
<i>Sheet 2 material</i>	2024-T3 ($E_{L_1} = 7240 \text{ daN/mm}^2$)
<i>Sheet 1 thickness</i>	1.27mm
<i>Sheet 2 thickness</i>	1.27mm
<i>Sheet Length</i>	150mm
<i>Clamping Length</i>	40mm
<i>Fastener</i>	Solid Type, one Manufactured round head (MS20470AD5-5)
<i>Fastener Material</i>	2017-T4 ($E_f = 7240 \text{ daN/mm}^2$)
<i>Hole Diameter</i>	4.0 mm
<i>Width</i>	5d = 20mm (1 line of fasteners)
<i>Rows</i>	2
<i>Pitch</i>	5d = 20mm
<i>Edge Distance</i>	2.5d = 10mm
<i>Head Diameter</i>	d_{head}/d

With all the described equations and methods for fastening stiffness it is possible to obtain a numerical value for the fastening stiffness using equation (3). It is then possible to compare the result to the stiffness found by using the equations of section 3.

5.1 Varying type of modelling and stiffness equation

The mesh of the plates is composed by square elements 2mm wide. The stiffness of the fastening was evaluated in four types of models:

- 1) Models with plates in the middle surface, resulting in an offset between the two plates corresponding to the sum of the thicknesses divided by two.

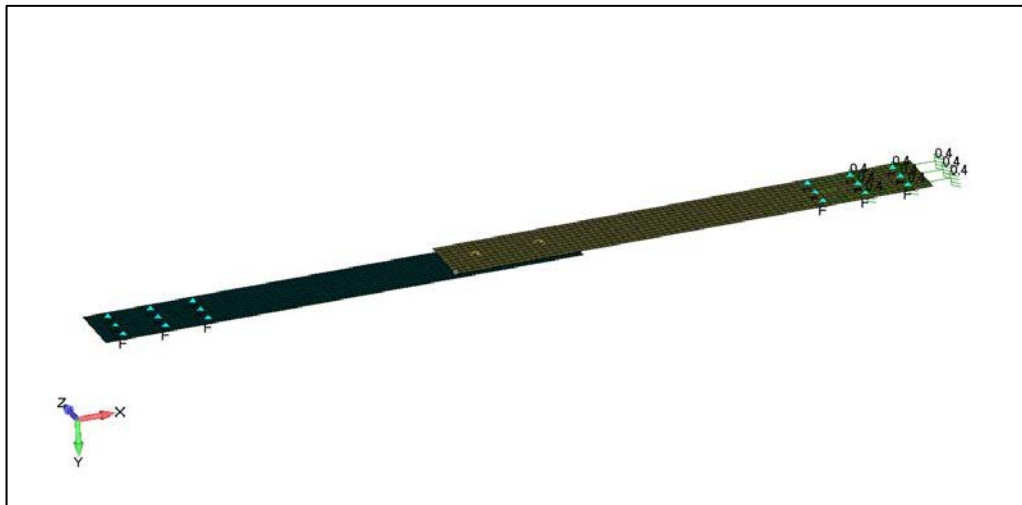


Figure 14: Model with plate offsets for the numerical experiment

- 2) Models with plates in the middle surface, resulting in an offset between the two plates corresponding to the sum of the thicknesses divided by two and a rigid element as described in section 1 to impose a no rotation condition. The model itself looks exactly like the one in Figure 14, except for the detail shown in figure Figure 4.
- 3) Models with plates without offset, making the spring length infinitesimal.



Figure 15: Model without plate offsets for the numerical experiment

4) Models with coplanar plates, with offset in the plate element itself.



Figure 16: Model with offset in the plate element for the numerical experiment

5) Rutman model.

The Rutman model consists in the one described in section 4 and it is shown in

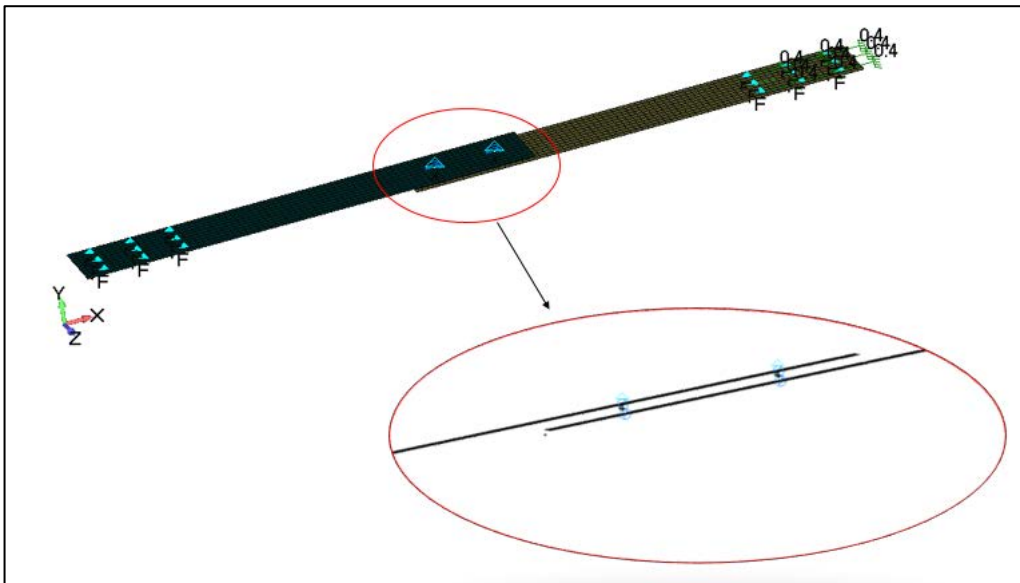


Figure 17: Rutman Model for the numerical experiment

For each model, a displacement of 0.4mm was prescribed in one end of the specimen and the total force was subsequently measured. The flexibility was computed using equation (3).

Table 2: Test Results Model with offset

<i>Model</i>	<i>F_x (daN)</i>	<i>f (mm/daN)</i>	<i>k (daN/mm)</i>	<i>Expected k (daN/mm)</i>
Grumman	191.433	0.00233	429.16	1214.66
Huth Rivet	209.6532	0.00197	508.40	2183.05
Huth Bolt	209.6532	0.00197	508.40	2192.27
Swift	215.8112	0.00186	538.19	2868.71
Tate	208.6012	0.00199	503.47	2094.57
Morris	192.30828	0.00231	432.69	1250.46
Rutman	231.20	0.00161	620.60	N/A

Table 3: Test Results Model with offset and a rigid element

<i>Model</i>	<i>F_x (daN)</i>	<i>f (mm/daN)</i>	<i>k (daN/mm)</i>	<i>Expected k (daN/mm)</i>
Grumman	179.15686	0.00262	382.19	1214.66
Huth Rivet	195.36467	0.00225	445.23	2183.05
Huth Bolt	195.36467	0.00225	445.23	2192.27
Swift	200.84193	0.00213	468.52	2868.71
Tate	194.42914	0.00227	441.36	2094.57
Morris	179.93614	0.00260	385.04	1250.46

Table 4: Test Results Model with no offset

<i>Model</i>	<i>F_x (daN)</i>	<i>f (mm/daN)</i>	<i>k (daN/mm)</i>	<i>Expected k (daN/mm)</i>
Grumman	281.1022	0.00100	1002.94	1214.66
Huth Rivet	322.2226	0.00063	1577.57	2183.05
Huth Bolt	322.2226	0.00063	1577.57	2192.27
Swift	337.0014	0.00053	1904.74	2868.71
Tate	319.744	0.00065	1531.09	2094.57
Morris	282.9936	0.00098	1022.44	1250.46

Table 5: Test Results Model with offset only in the shell elements

<i>Model</i>	<i>Fx (daN)</i>	<i>f (mm/daN)</i>	<i>k (daN/mm)</i>	<i>Expected k (daN/mm)</i>
Grumman	191.43476	0.00233	429.17	1214.66
Huth Rivet	209.6554	0.00197	508.41	2183.05
Huth Bolt	209.6554	0.00197	508.41	2192.27
Swift	215.8134	0.00186	538.20	2868.71
Tate	208.6032	0.00199	503.48	2094.57
Morris	192.31004	0.00231	432.70	1250.46

Table 2 through Table 5 shows that for the refined mesh (2mm wide), the measured stiffness is always lower than the expected. Thus, the model is softening the fastening. In the next section, it will be measured how much the mesh increases joint flexibility.

5.2 Varying the mesh size

By varying the mesh size, it can be verified that it is as important as the method of modelling the joint. The models compared are the models with offset from Rutman and Morris. The setup of the test is shown in Table 1.

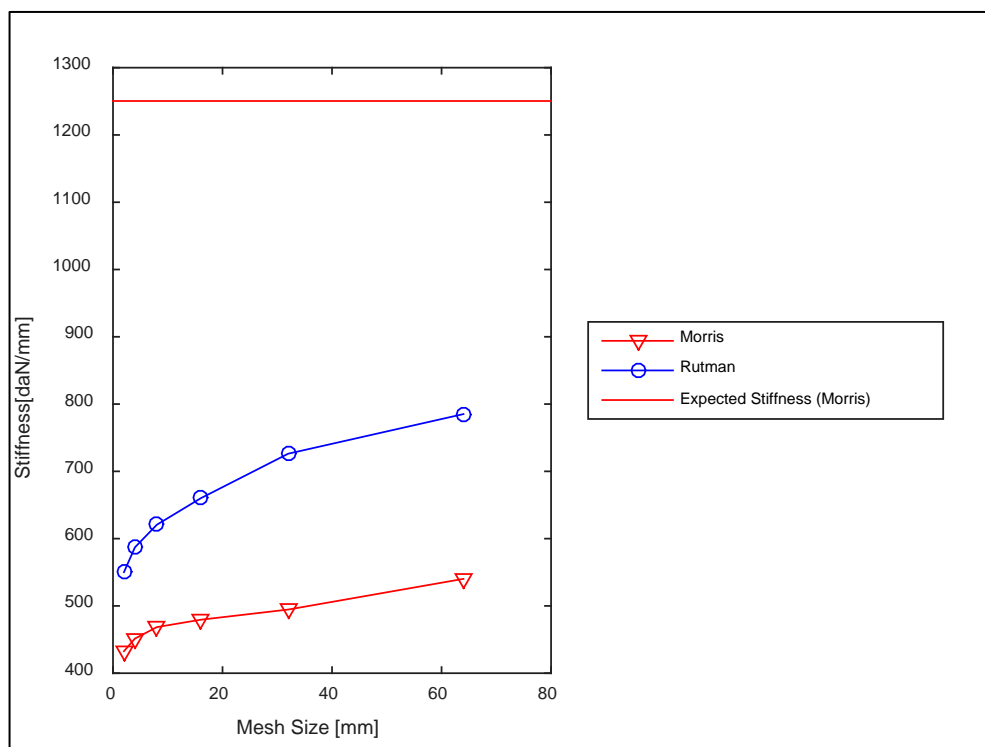


Figure 18: Variation of the fastening stiffness with the mesh size

As shown by Figure 18, the variation of the stiffness with the mesh size is significant for meshes smaller than 8mm. Thus, it can be concluded that an over-refined mesh can lead to a more flexible model. In chapter 6, the results will be compared with empirical data (the 8mm model will be used).

6. Comparison with empirical results

In his PhD thesis, Morris made available part of the raw data. He performed the cyclic test as described by Huth, and measured the flexibility in the cycle in which the force is $2/3$ of the maximum. He performed tests for a series of specimen with 2 fastener rows. It was possible to verify the influence of sheet thickness, material, hole expansion and other factors. In one series of experiments, the influence of the number of rows in the flexibility was verified. The same set-up of the base experiment shown in Table 1 was used, but with 1, 3 and 4 rows of fasteners. Those are more suitable to describe the change in the modelling aspects. On the other hand, the tests with three and four rows lead to no failure due to incapacity of the machine. This can lead to an imprecision to the application of the method proposed by Huth. Since the maximum force is estimated, the loop is also an estimation. But this inaccuracy is also present on the Morris equation of flexibility.

- 1 Row of fasteners

Figure 19 shows the finite element model of a lap joint tested by Morris. The full range of the test performed is showed right below (Figure 20).

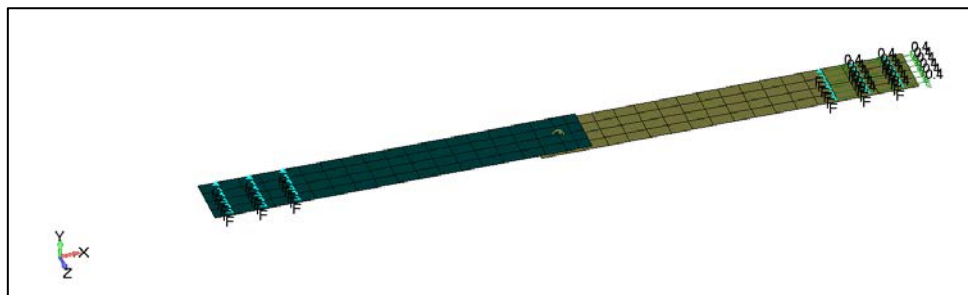


Figure 19: Finite element model of a single row lap joint

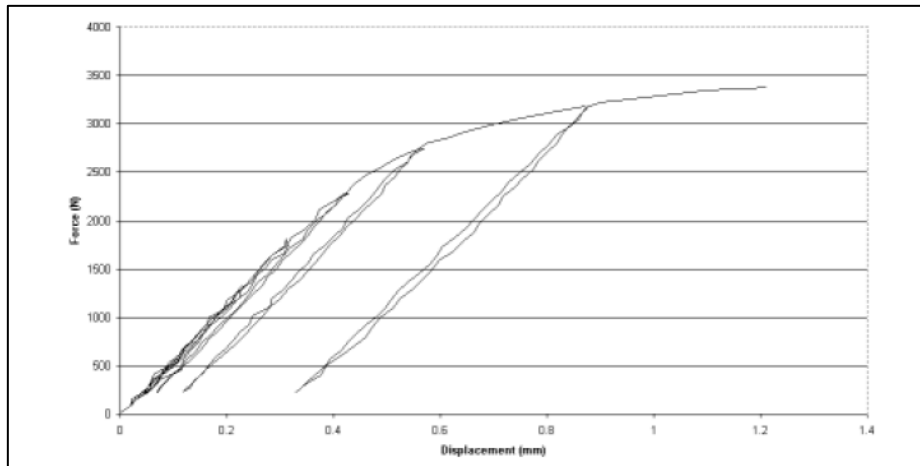


Figure 20: Test for a lap joint with 1 row of fasteners, described in Table 1 (Morris)

By modelling the fastener using both single-spring (Morris) and multi-spring approaches it is possible to compare the numerical and experimental tests.

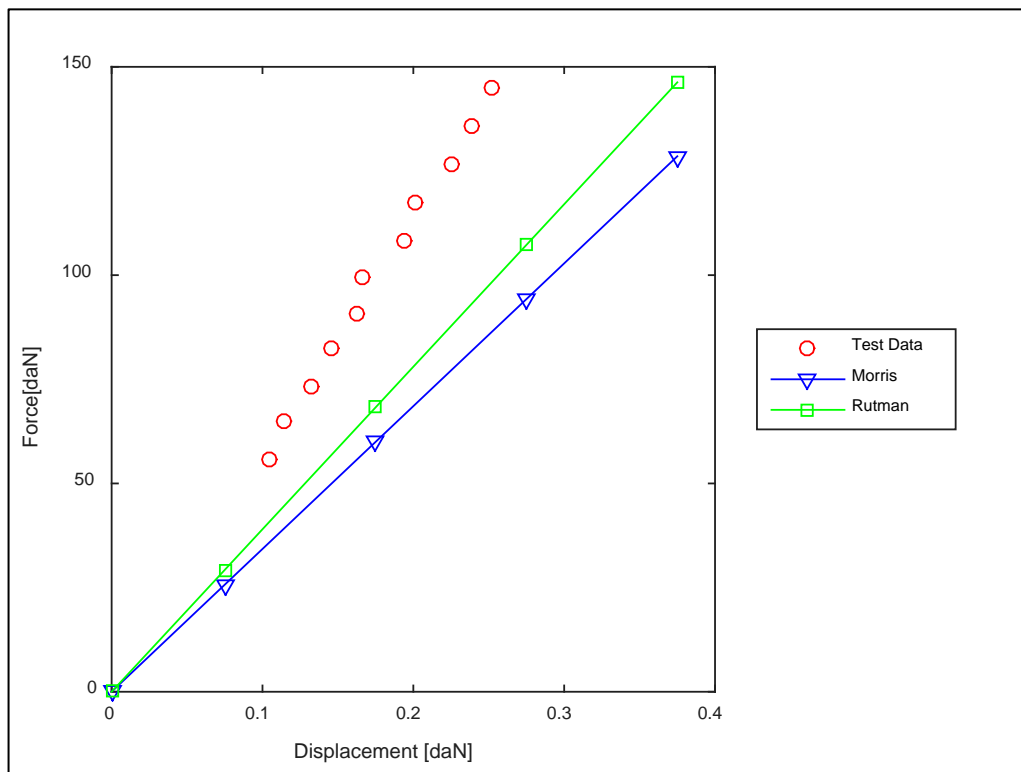


Figure 21: Comparison between the finite element model using Morris and Rutman approaches and the Test Data for 1 row of fasteners

As can be seen by Figure 21, the finite element model for 1 row of fasteners is much more flexible than the experimental result.

- 2, 3 and 4 Rows of fasteners

The same procedure was performed for 2,3 and 4 rows of fasteners. The results are shown below:

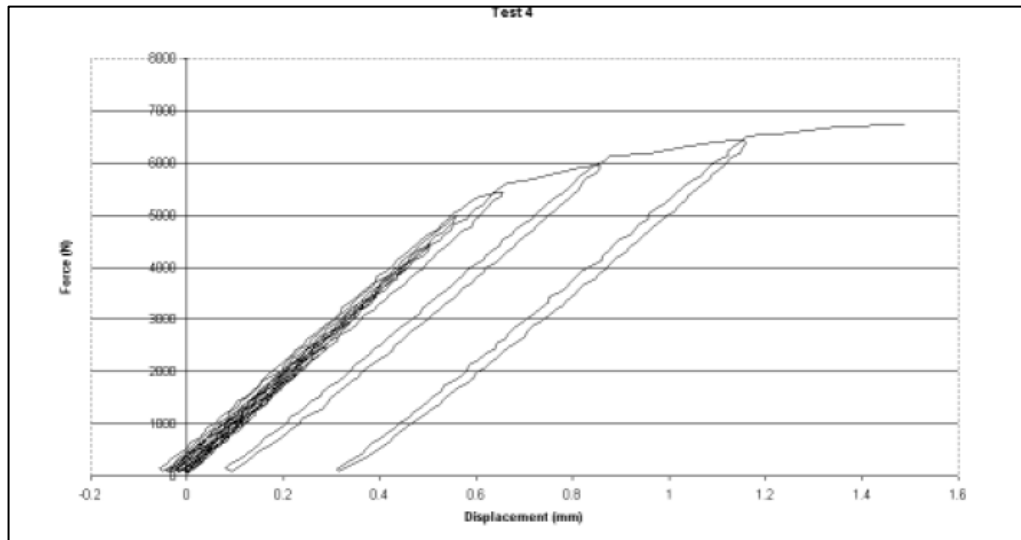


Figure 22: Test for a lap joint with 2 rows of fasteners, described in Table 1 (Morris).

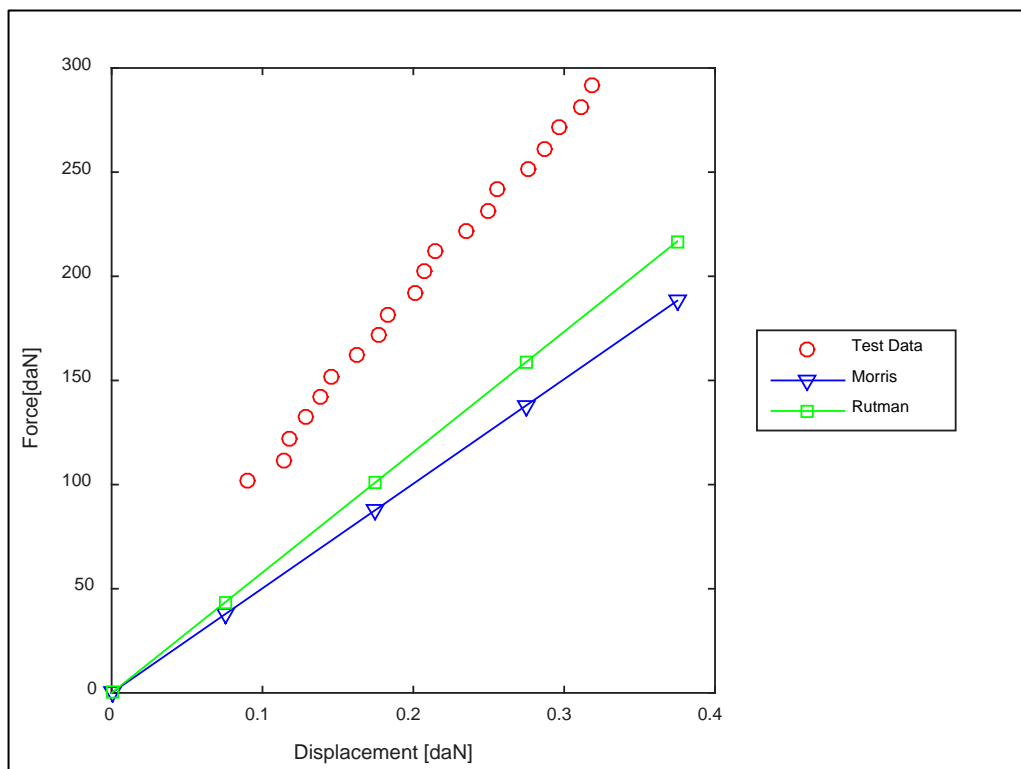


Figure 23: Comparison between the finite element model using Morris and Rutman approaches and the Test Data for 2 rows of Rivets.

The result for 2 rows of fasteners is also a crude approximation for both methods.

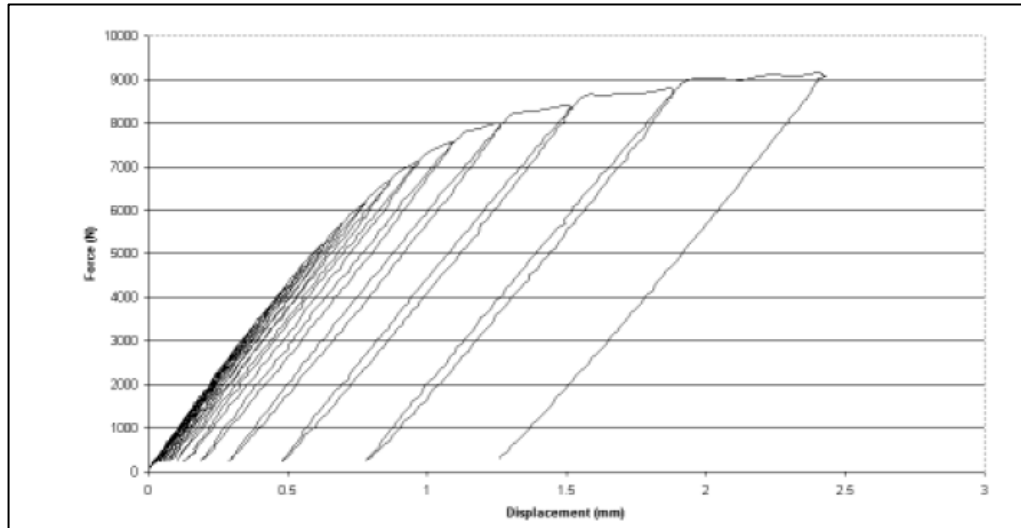


Figure 24: Test for a lap joint with 3 rows of fasteners, described in Table 1 (Morris)

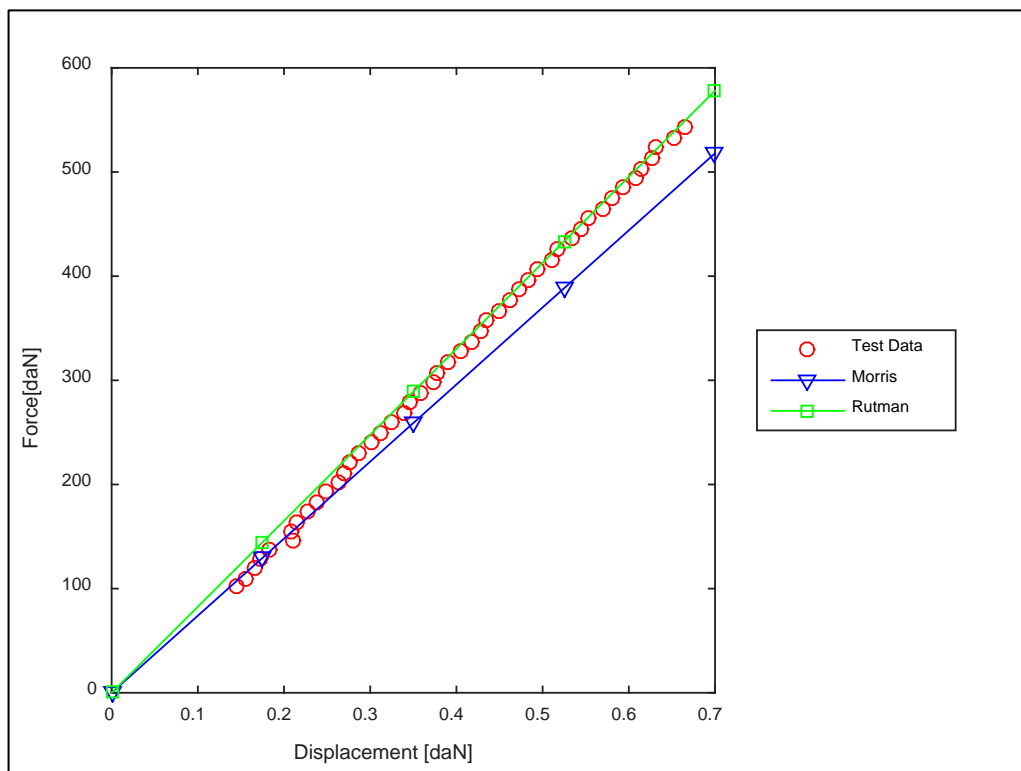


Figure 25: Comparison between the finite element model using Morris and Rutman approaches and the Test Data for 3 rows of Rivets

For three rows of rivets, the results are excellent for the Rutman approach. The result was also close by using Morris' single spring method.

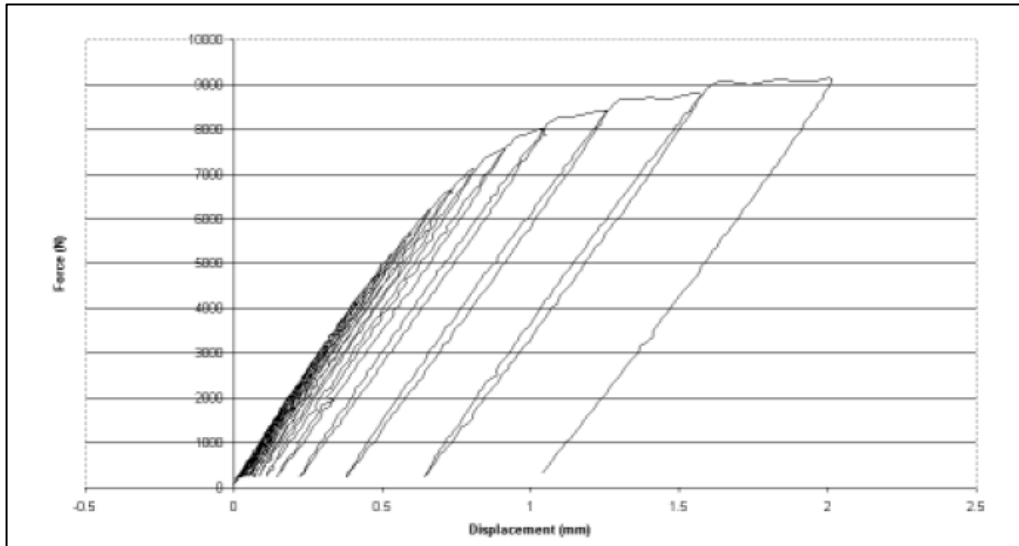


Figure 26: Test for a lap joint with 4 rows of fasteners, described in Table 1 (Morris)

In the fourth test, there was significant plastic deformation, so the original data, published by Morris, was subtracted by the permanent deformation.

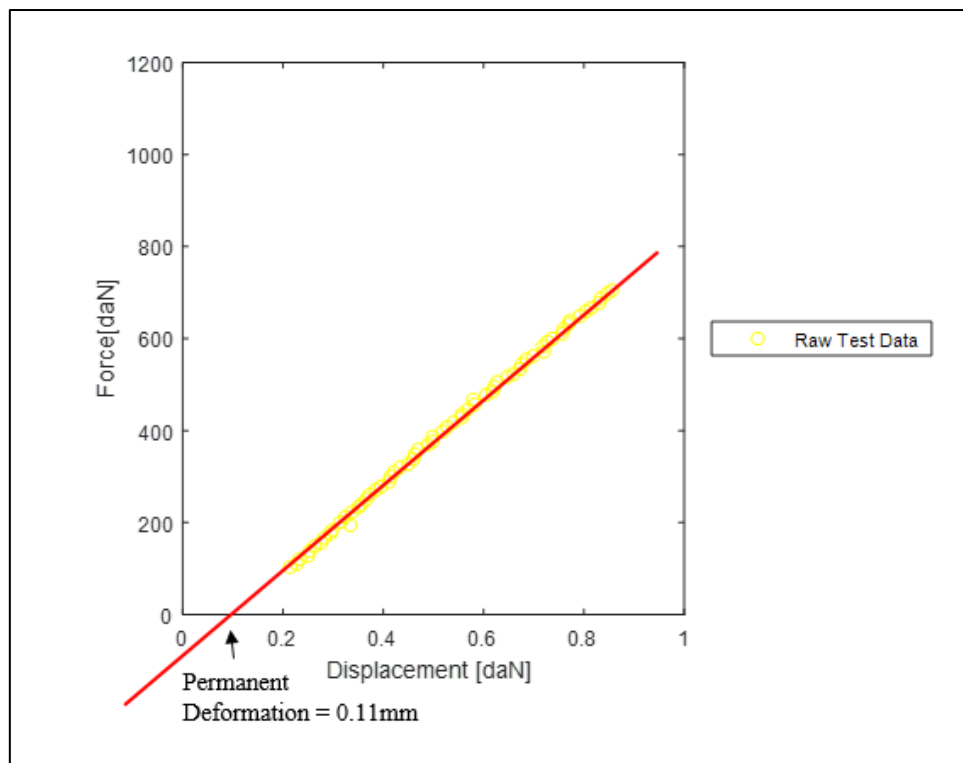


Figure 27: Plastic deformation of the fourth test

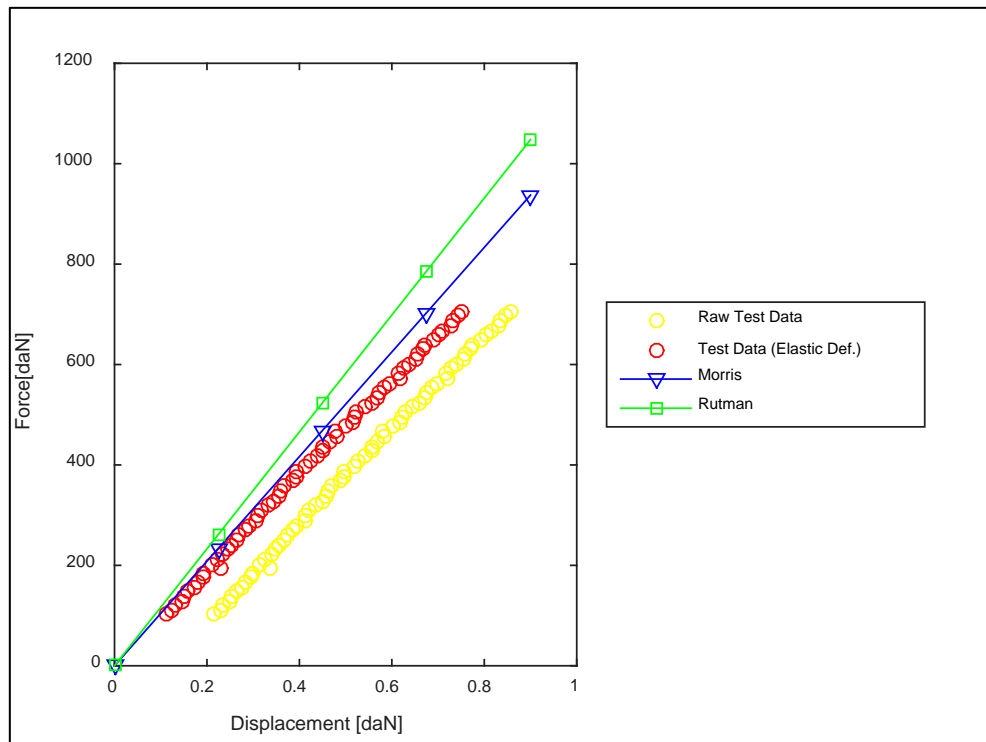


Figure 1: Comparison between the finite element model using Morris and Rutman approaches and the Test Data for 4 rows of fasteners

The results are also good for 4 rows of fasteners. In this case, Morris is closer to the result than Rutman.

The results indicate that as the number of rows of fasteners is increased, the finite element model becomes closer to the real structure. This can be explained by an unrealistic secondary moment that generates up to 1.3mm of vertical displacement in the first model, as shown in Figure 28.

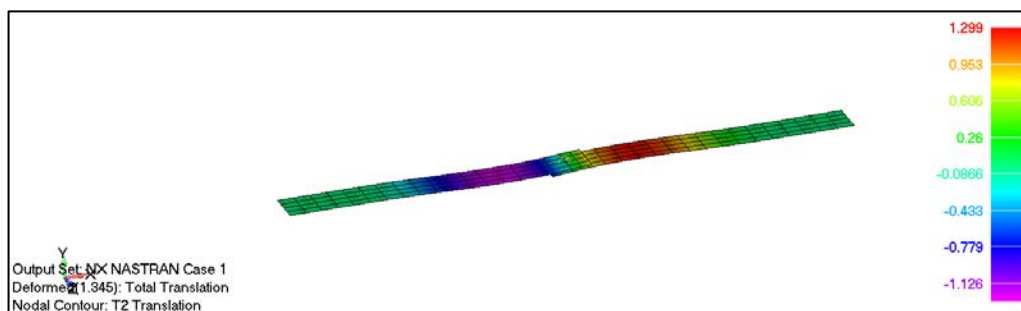


Figure 28: Vertical Displacement of the 1 row test finite element model

As the number of rows increases, this effect is decreased, especially in the Rutman approach, which has compatibility elements, that prevent the plate elements close the fastening from rotating with respect to each other (Rutman, 2000).

7. Conclusions

The results found in this paper show that modelling fastening by discrete elements can introduce substantial errors in the model, when it comes to determining the proper stiffness.

The comparison between single spring or multi-spring approaches showed similar results. The advantage that was not mentioned yet is that, in the multi-spring approach, no test was necessary to develop the theory. The Morris equation considers several joint parameters that can be hard to be implemented in a FEM pre-processor program.

For larger models, the Rutman model is expected to behave even better, making the load transfer more realistic. Hence, for large models in which the fastening must be all modelled (a composite wing or empennage for example), the author recommends the usage of the Rutman model.

For smaller models, the Morris equation is recommended, but the spring must be infinitesimal in size and the plate elements of the joint must be in the same plane.

8. References

Huth, Heimo (1985). *Influence of fastener flexibility on the prediction of load transfer and fatigue life for multiple-row joints*. Fatigue in Mechanically Fastened Composite and Metallic Joints. Proceedings of the Symposium. 30 pages.

Morris, George (2004). *Defining a standard formula and test-method for fastener flexibility in lap-joints*: PhD Thesis, Technical University Delft. 127 pages.

Rutman, Alexander (2000). *Fasteners Modeling for MSC.Nastran Finite Element Analysis*: World Aviation Conference. 19 pages.

Rutman, Alexander (2009). *Fastener Modeling for Joining Composite Parts*: Americas Virtual Product Development Conference. 28 pages.

M.E. Grayley (2001), ESDU – 98012 - *Flexibility of, and load distribution in, multi-bolt lap joints subject to in-plane axial loads*: Engineering data Sciences Data Unit. 50 pages.

MSC.Software Corporation (2010), *MD/MSC Nastran Quick Reference Guide*, 3422 pages.

Swift, T. (1971), *Development of Fail-Safe Design Features of the DC-10*: ASTM, STP 486, pp.164-214, 1091. 50 pages.

Tate, M.B., Rosenfeld, S.J. (1946), *Preliminary Investigation on Loads Carried by Individual Joints*, NACA-TN-1051. 74 pages.